Phase Transformations in Free Films

John Nayar

A dissertation submitted in partial fulfillment of
the requirements for the degree of

Master of Science in Mechanical Engineering

University of Washington

2012

Reading Committee:

Lucien N. Brush, Chair

Alberto Aliseda

James Riley

Program Authorized to Offer Degree:
UW Mechanical Engineering

University of Washington

Abstract

Phase Transformations in Free Films

John Nayar

Chair of the Supervisory Committee:
Associate Professor Lucien N. Brush
Department of Material Sciences and Engineering

The purpose of this dissertation is to present the derivation of the governing equations for a free-film undergoing phase separation using a long-wavelength approximation to the Navier-Stokes equations coupled with the Cahn-Hilliard equation for phase transformation in a binary liquid. The equations are derived for two cases, one where the diffuse interphase boundary is assumed to have a thickness larger than the film thickness and the other where it is assumed to be less than the film thickness. A linear stability analysis is performed for these two cases and the conditions for instability are examined. An equation describing the profile of the interphase boundary for the case where the interphase boundary thickness is less than the film thickness is also derived assuming a no-flow condition, using a matched asymptotic analysis.

Typically one of the liquid phases will wet the gas-liquid interface. Therefore, another aim is to numerically simulate the phenomenon of the wetting in a free-film by one of the binary liquid phases. This is done in a one-dimensional case as well as for an axisymmetric cylindrical geometry. Finally, the effect of the free-film thickness on the wetting behavior of the phase boundary liquid phases along the film interface is investigated using numerical methods. It is shown that as the film thickness is gradually reduced, the wetting along the interface disappears.

TABLE OF CONTENTS

LIST OF FIGURES

ACKNOWLEDGMENTS

First and foremost, I would like to convey my deepest gratitude to my advisor Dr. Lucien Brush for his continual guidance, patience, support and for always being available on Skype.

I would also like to express my appreciation to my Committee members Dr. James Riley and Dr. Alberto Aliseda for their encouragement.

I would like to thank my friends spread all around the world for all their support and encouragement.

This thesis would not have been possible without the loving support of my parents to whom I am very grateful. I would also like to thank my sister, my in-laws and other members of my family who believed in me.

Last but not the least, I wish to thank God for giving me the strength and motivation to finish off what I started.

DEDICATION

to anyone who believes in the magic of last minute work

and to my dear wife, Emma

Chapter 1

INTRODUCTION

A free-film is a thin layer of liquid bounded by gas phases on either side. A good example of free-films are foams, where the gas bubbles are formed on or in a liquid. The bubbles are separated from each other by liquid films. Metallic foams, due to their characteristics of high stiffness, low specific weight, high compression strength, and high-impact energy absorption combined are useful for structural and load bearing applications[1]. They are also being considered as potential materials in the automobile and aerospace industries, where their specific structure makes them useful for light-weight construction or crash energy absorption[2]. A thin-film, on the other hand, is a thin layer of liquid lying on a substrate. Although this work focuses on free-films and extensional flow, there has been lots of research focused on the dynamics of thin-films and the lubrication flow. The applications of thin-films range from nucleate boiling[3], coating processes such as spin coating[4], dip coating, metered coating, transfer coating, condensate motion on heat exchangers, and even the movement of contact lenses in medicine[5]. It is important to acknowledge the research carried out in thin-films because some of the phenomena observed are also important in free-films. However, the flow and interface evolution are governed by different sets of equations and the balance of forces are also different in the high-aspect ratio limit. See for example Oron *et al.*[6] and references therein.

A great deal of study has been done in the past on the evolution equations and stability of a free-film. Erneux and Davis used long-wave asymptotics to derive evolution equations for a viscous free-film subject to van der Waals attractions and for the first time obtained an analytical estimate for film rupture[7]. Oron, Bankoff and Davis derived the evolution equations for thin and free-films using a long-wave theory. They derived the equations for particular cases to include various physical parameters and discussed the linear stability properties of the base-state solutions and the non-linear spatiotemporal evolution of the

interface for these cases[6]. De Wit, Gallez and Christov derived three non-linear evolution equations to study the dynamics of a free-liquid film with insoluble surfactants all the way up to film rupture. They included the effects of van der Waals attraction, capillary forces, and Marangoni forces and performed a linear stability analysis to show how these parameters affected the rupture time. They also showed that the surfactant monolayer has a stabilizing effect on the growth of the instability[8]. Tabakova and Radev examined the linear stability of a 1-D free-film attached on a rectangular frame with a prescribed wetting angle surrounded by an ambient gas. They solved a non-linear system for the longitudinal velocity and film thickness using differential Gauss elimination[9]. Tabakova showed that for this case, the film rupture can be caused either by the non-existence of a static film shape or by the instability of an existing static shape[10]. Sharma, Kishore, Salaniwal and Ruckenstein studied the non-linear long-wave stability of free-films based on numerical solutions, and also developed a weakly non-linear theory. They predicted that the Lifshitz-van der Waals forces, inertia and mode interactions are greatly enhanced if the initial amplitude is large and that this may cause linearly stable disturbances to engender strong subcritical instabilities and film rupture[11]. Prevost and Gallez derived an evolution equation describing the variation of the film thickness along the lateral space dimension for the squeezing mode and predicted the influence of non-linearities on the rupture of the free-film for the first time. They showed that the presence of non-linearities significantly accelerates rupture of the film[12]. Dai and Leal proposed a disjoining pressure pertaining to van der Waals attractive forces for a film of non-uniform thickness. They derived this by minimizing the total Helmholtz free energy for a thin-film residing on a solid substrate[13]. Thiele, Madruga and Frastia derived transport equations using non-equilibrium thermodynamics to describe the coupled decomposition and profile evolution of a thin-film of binary mixture[14] and the linear stability of the film was also studied showing the effects of increasing the film thickness on the stability for the cases of diffusive and convective transport for different cases of energetic bias at the surfaces[15]. Thiffeault and Naraigh presented a long-wavelength approximation to the Navier-Stokes coupled Cahn-Hilliard equations for phase separation in thin-films to derive a couple of evolution equations, one for the free surface and another for concentration. They treated the interphase boundary

to be diffuse in nature and demonstrated that the film does not rupture in the presence of a repulsive substrate-film interaction potential[16].

Inspired by the above work, *chapter 2* of this dissertation derives the evolution equations for a free-film undergoing phase transformation. The derivations are carried out for a two-dimensional symmetric case. The binary fluid components are density and viscosity matched and the derivation includes contributions due to the capillary forces and van der Waals attractions. The surface tension gradients along the interfaces are assumed to be zero, and thus Marangoni effects are not included. A long-wavelength approximation is applied to the coupled Navier-Stokes and Cahn-Hilliard equations which simplifies the system of equations and ultimately reduces it to three equations. The evolution equations are derived for two cases, i.e. for two different scalings of the interphase boundary. The first scaling assumes the interphase boundary thickness to be smaller than the film thickness, whereas the second scaling assumes the opposite. A linear stability analysis is carried out to examine the stability of the film for each case. The profile of the interphase boundary in a two-phase fluid mixture is also derived for the case in which the interphase boundary is smaller than the film thickness for a no-flow case, by using a matched asymptotic analysis.

Pioneering work has been done by Cahn on the thermodynamics and kinetics of phase transitions and interfacial phenomena. Cahn and Hilliard studied the stability of a two-component binary solution and investigated whether nucleation is the mechanism for phase transformation or spinodal decomposition[17]. Moreover, Cahn showed that in a binary fluid near its critical point, one of the binary liquid (critical) phases completely wets the third solid phase even when the phase is no longer stable in the bulk[18]. The transition from complete to partial wetting of the third phase by one of the critical phases was illustrated by Moldover and Cahn[19]. Tarazona, Telo Da Gama and Evans showed that in a binary fluid mixture, the transition from partial to complete wetting of the third phase by one of the phase-separated fluids can be a first-order surface transition as predicted by Cahn or a second-order surface phase transition[20]. Hadjiagapiou and Evans showed that for a model binary fluid which exhibits a liquid-liquid upper critical point on a solid substrate, the solid-vapor interface can be wet by a wetting film composite of both phase-separated liquids[21]. Wensink and Jerome looked at the stability with respect to dewetting of stable thin-films

on a substrate due to density fluctuations. They showed that the film ruptures into droplets if sufficiently large density fluctuations appear in the film[22]. Wang, Composto, Hobbie and Han used composite profiling and surface-imaging techniques to see the effects of phase separation, wetting and capillary instabilities in thin polymer films with short and long-wavelength modes[23]. Genzer and Kramer studied the transitioning from three layers to two layers in a binary mixture of immiscible polymers on a substrate by increasing the surface energy of the substrate[24].

Chapter 3 of this dissertation deals with the numerical simulation of the phenomenon of wetting of one phase in a two-phase binary liquid solution in a free-film. The simulations are carried out for a symmetric 1-D case and an axisymmetric cylindrical case. Cahn and Hilliard derived an expression for the free energy of a non-uniform system in terms of the composition of one of the components as $N_v \int_v \left[f_0(c) + K(\nabla c)^2 \right] dv$, where N_v is the number of molecules per unit volume, ∇c is the concentration gradient, f_0 is the free energy of a molecule for a homogeneous system and K is a positive constant[25]. Using this, Cahn gave another expression for the excess free energy of unit area of surface due to the free energy contribution from a solid surface[18]. The latter expression is minimized in the numerical simulations to determine the composition of the free-film. In his thorough presentation of the statics and dynamics of wetting, de Gennes describes Cahn's model and he chooses a quadratic approximation for the free surface interaction free energy[26]. For simplicity, a quadratic approximation to the surface free energy has been used in this paper as well. The calculations are constrained by a conservation of mass condition required since the domain of the system in consideration is finite. The conditions denoting the transition from wetting to non-wetting behavior is calculated and the effect of the thickness of the free-film is examined. It is shown that the wetting at the phase boundary *disappears* as the film progressively becomes thinner and thinner.

Chapter 2

DERIVATION OF THE CAHN-HILLIARD NAVIER STOKES EQUATIONS FOR A FREE-FILM

2.1 The model

The evolution equations for a free-film undergoing phase separation are derived for a two-dimensional case. The free-film geometry is symmetric about the z=0 axis as seen in Figure 2.1. The thickness of the film extends from $z = -h$ to $z = +h$. The phase separated components are assumed to have identical density and viscosity. The coupled equations governing the flow and phase separation in a binary liquid solution are:

$$\frac{\partial v}{\partial t} + v.\nabla v = \nabla.T - \frac{1}{\rho}\nabla\phi; \tag{2.1}$$

$$\frac{\partial c}{\partial t} + v.\nabla c = D\nabla^2(c^3 - c - \gamma\nabla^2 c); \tag{2.2}$$

$$\nabla.v = 0, \tag{2.3}$$

where $T_{ij} = \frac{p}{\rho}\delta_{ij} + \nu\left(\frac{\partial v_i}{\partial x_j} + \frac{\partial v_j}{\partial x_i}\right) - \beta\gamma\frac{\partial c}{\partial x_i}\frac{\partial c}{\partial x_j}$ is the stress tensor, v is the fluid velocity, ρ is the density of the fluid, ϕ is a body potential, c is the dimensionless concentration (where $c = \pm 1$ pertains to each of the two phases), D is the diffusion coefficient with units $[length]^2[time]^{-1}$, $\sqrt{\gamma}$ is a constant that gives the typical width of the interphase boundary, p is the pressure, ν is the kinematic viscosity, μ is the dynamic viscosity ($\nu = \frac{\mu}{\rho}$) and β is a constant with units $[energy][mass]^{-1}$.

The boundary conditions of the symmetry plane at $z = 0$ are

$$u_z = 0; \tag{2.4a}$$

$$w = 0; \tag{2.4b}$$

$$c_z = 0; \tag{2.4c}$$

$$\text{and} \quad c_{zzz} = 0. \tag{2.4d}$$

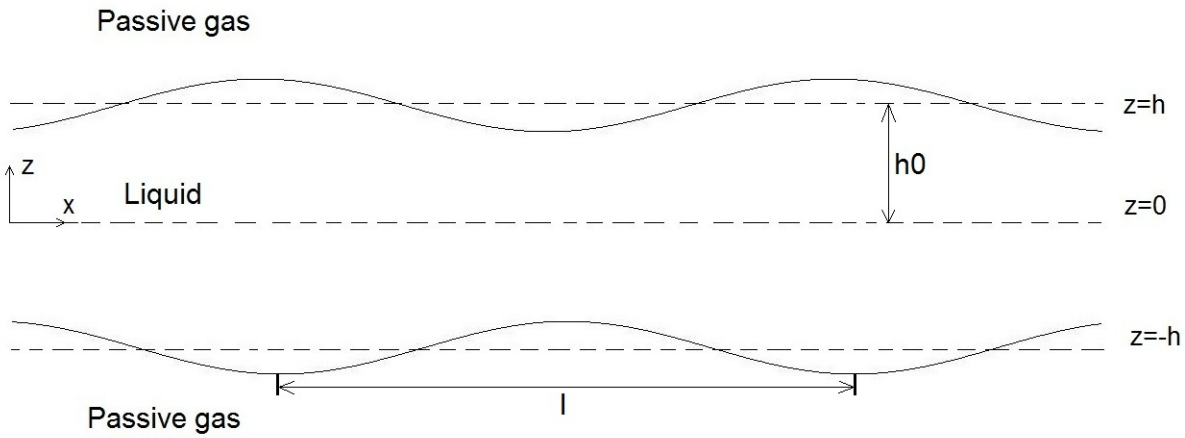

Figure 2.1: Sketch of a free-film symmetric about z=0

On the free surface at $z = h(x,t)$, the interfacial conditions are:

$$\hat{n_i}\hat{n_j}T_{ij} = -\sigma\kappa \tag{2.5}$$

$$\text{and} \quad \hat{n_i}\hat{t_j}T_{ij} = -\frac{\partial\sigma}{\partial s}, \tag{2.6}$$

where $\hat{n} = \dfrac{(-h_x, 1)}{[1 + {h_x}^2]^{1/2}}$ is the unit normal to the surface, $\hat{t} = \dfrac{(1, h_x)}{[1 + {h_x}^2]^{1/2}}$ is the unit vector tangent to the surface, s is the surface coordinate, σ is the surface tension and κ is the mean curvature given as $\kappa = \nabla.\hat{n} = \dfrac{h_{xx}}{[1 + {h_x}^2]^{3/2}}$.
The kinematic boundary condition preventing any flow through the free surface is

$$w = \frac{\partial h}{\partial t} + u\frac{\partial h}{\partial x}. \tag{2.7}$$

And finally, the boundary conditions for concentration at the free-film surface are:

$$\hat{n_i}\partial_i c = 0 \tag{2.8}$$

$$\text{and} \quad \hat{n_i}\partial_i\nabla^2 c = 0. \tag{2.9}$$

The boundary conditions chosen satisfy the total mass and volume conservation conditions for the system, mass $= \int_{Dom(t)} dxdzc(x,z,t)$; Volume$= \int_{Dom(t)} dxdz$, where $Dom(t)$ represents the time-dependent domain of integration.

2.2 Scaling of variables

A long-wavelength approximation is assumed for the system of equations because the thickness of the film is much smaller than its lateral dimension ($h << l$). This fact may be exploited to greatly simplify the governing equations. Toward this end, the small parameter 'δ' is defined as $\delta = \frac{h_0}{l}$, where h_0 is the mean half-thickness of the free-film and l is the lateral dimension of the film. All variables are rescaled according to the following definitions. Upper-case letters are used for the non-dimensionalized parameters and lower-case letters are used for the dimensional parameters. The lateral dimension representing the length of the film $X = \frac{x}{l}$; the vertical dimension representing the thickness of the film $Z = \frac{z}{h_0}$, Z extends from $-H$ to $+H$ where $H = \frac{h}{h_0}$; the diffusion time scale $t_0 = \frac{l^2}{D} = \frac{h_0^2}{\delta^2 D}$ which gives $T = \frac{t}{\left(h_0^2/\delta^2 D\right)}$; and the fluid velocity scale in the $x-$direction $= u_0 = \frac{l}{t_0} = \frac{\delta D}{h_0}$ which gives $U = \frac{u}{(\delta D/h_0)}$. From the continuity equation, the scaling for the velocity in the $z-$direction, w_0 is determined, $\frac{h_0}{\delta D}\frac{\partial u}{\partial x} l + \frac{\partial W}{\partial z} h_0 = 0$ giving $W = \frac{w h_0}{\delta^2 D}$. Anticipating that the flow will be locally parallel, i.e. $\mu u_{zz} = p_x$, the scaling for the pressure is found as $P_0 = \frac{\mu D}{h_0^2}$ and thus $P = \frac{p}{\left(\mu D/h_0^2\right)}$.
These scalings lead to a non-dimensional form of stress tensor given by:

$$T = \begin{bmatrix} -\frac{\mu D}{\rho h_0^2} P + 2\nu \frac{\delta D}{h_0 l}\frac{\partial U}{\partial X} - \frac{\beta\gamma}{l^2}\left(\frac{\partial c}{\partial X}\right)^2 & \nu\left(\frac{\delta D}{h_0^2}\frac{\partial U}{\partial Z} + \frac{\delta^2 D}{h_0 l}\frac{\partial W}{\partial X}\right) - \frac{\beta\gamma}{l h_0}\frac{\partial c}{\partial X}\frac{\partial c}{\partial Z} \\ \nu\left(\frac{\delta D}{h_0^2}\frac{\partial U}{\partial Z} + \frac{\delta^2 D}{h_0 l}\frac{\partial W}{\partial X}\right) - \frac{\beta\gamma}{l h_0}\frac{\partial c}{\partial X}\frac{\partial c}{\partial Z} & -\frac{\mu D}{\rho h_0^2} P + 2\nu \frac{\delta^2 D}{h_0^2}\frac{\partial W}{\partial Z} - \frac{\beta\gamma}{h_0^2}\left(\frac{\partial c}{\partial Z}\right)^2 \end{bmatrix}$$

The unit normal and the tangent vectors in non-dimensionalized forms are given by:

$$\hat{n} = \frac{(-\delta H_X, 1)}{\left[1 + \delta^2 {H_X}^2\right]^{1/2}}; \quad \hat{t} = \frac{(1, \delta H_X)}{\left[1 + \delta^2 {H_X}^2\right]^{1/2}}.$$

In the same way, the dimensionless mean curvature $\kappa = \frac{\delta H_{XX}}{l\left[1 + \delta^2 {H_X}^2\right]^{3/2}}$.

Because the thicknesses of the films considered are less than $\sim 200\ nms$, the effect of van der Waals forces needs to be included. Defining the body force ϕ as van der Waals force, $\phi = \dfrac{A}{(2h)^3}$, then an appropriate scaling requires ϕ to be $O(\delta^2)$. Here, $A = \dfrac{\delta^2 A'}{6\pi h_0 \rho \nu^2}$, where A' is the Hamaker constant. ϕ is dependent on x and independent of z. Define $\phi = \delta^2 \Phi$, where $\Phi \sim O(1)$.

The non-dimensional equations governing flow are now written as:

$$\delta^2 Re\left[\frac{\partial U}{\partial T} + U\frac{\partial U}{\partial X} + W\frac{\partial U}{\partial Z}\right] = -\frac{\partial}{\partial X}(P + \delta^2\Phi) + \delta^2\frac{\partial^2 U}{\partial X^2} + \frac{\partial^2 U}{\partial Z^2} - \frac{1}{2}\frac{\beta\gamma}{\nu D}\frac{\partial}{\partial X}\left[\delta^2\left(\frac{\partial c}{\partial X}\right)^2 + \left(\frac{\partial c}{\partial Z}\right)^2\right] - \frac{\beta\gamma}{\nu D}\frac{\partial c}{\partial X}\left[\delta^2\frac{\partial^2 c}{\partial X^2} + \frac{\partial^2 c}{\partial Z^2}\right] \quad (2.10)$$

$$\delta^4 Re\left[\frac{\partial W}{\partial T} + U\frac{\partial W}{\partial X} + W\frac{\partial W}{\partial Z}\right] = -\frac{\partial P}{\partial Z} + \delta^4\frac{\partial^2 W}{\partial X^2} + \delta^2\frac{\partial^2 W}{\partial Z^2} - \frac{1}{2}\frac{\beta\gamma}{\nu D}\frac{\partial}{\partial Z}\left[\delta^2\left(\frac{\partial c}{\partial X}\right)^2 + \left(\frac{\partial c}{\partial Z}\right)^2\right] - \frac{\beta\gamma}{\nu D}\frac{\partial c}{\partial Z}\left[\delta^2\frac{\partial^2 c}{\partial X^2} + \frac{\partial^2 c}{\partial Z^2}\right] \quad (2.11)$$

$$\frac{\partial U}{\partial X} + \frac{\partial W}{\partial Z} = 0. \quad (2.12)$$

The equation governing compositional changes and phase transformations in the bulk liquid is:

$$\delta^2\left[\frac{\partial c}{\partial T} + U\frac{\partial c}{\partial X} + W\frac{\partial c}{\partial Z}\right] = \delta^2\frac{\partial^2}{\partial X^2}(c^3 - c) + \frac{\partial^2}{\partial Z^2}(c^3 - c) - \delta^4 C_n^2\frac{\partial^4 c}{\partial X^4} - C_n^2\frac{\partial^4 c}{\partial Z^4} - 2\delta^2 C_n^2\frac{\partial^2}{\partial X^2}\frac{\partial^2 c}{\partial Z^2}, \quad (2.13)$$

where the Reynolds number is given by $Re = \dfrac{u_0 l}{\nu} = \dfrac{D}{\nu} \sim O(1)$ and $C_n^2 \equiv \dfrac{\gamma}{h_0^2}$.

The boundary conditions in the non-dimensionalized form are as follows.

At $Z = \pm H$, the normal component of the stress tensor obeys:

$$\delta^2\left(\frac{\partial H}{\partial X}\right)^2\left[-P + 2\delta^2\frac{\partial U}{\partial X} - B\delta^2\left(\frac{\partial c}{\partial X}\right)^2\right] \mp 2\delta^2\frac{\partial H}{\partial X}\left[\frac{\partial U}{\partial Z} + \delta^2\frac{\partial W}{\partial X} - B\frac{\partial c}{\partial X}\frac{\partial c}{\partial Z}\right] - P + 2\delta^2\frac{\partial W}{\partial Z} - B\left(\frac{\partial c}{\partial Z}\right)^2 = \delta^3\left(\frac{\sigma l}{\nu D}\right)\frac{H_{XX}}{\left[1 + \delta^2 {H_X}^2\right]^{1/2}}, \quad (2.14)$$

where $B = \dfrac{\beta\gamma}{\nu D}$. Also, here $\left(\dfrac{\sigma l}{\nu D}\right) = Ca^{-1}$, where Ca is the Capillary number. This is rescaled as $\tilde{Ca} = \delta^{-1}Ca$, where $Ca \sim O(1)$ so that the RHS is now $\dfrac{-\delta^2 \tilde{Ca}^{-1} H_{XX}}{[1+\delta^2 {H_X}^2]^{1/2}}$. The tangential component of the stress tensor obeys:

$$
\begin{aligned}
&-\delta^2 \frac{\partial H}{\partial X}\left[2\frac{\partial U}{\partial X} - B\left(\frac{\partial c}{\partial X}\right)^2\right] \pm \left(\frac{\partial U}{\partial Z} + \delta^2 \frac{\partial W}{\partial X}\right) \mp B \frac{\partial c}{\partial X}\frac{\partial c}{\partial Z} \\
&\quad \mp \delta^2 \left(\frac{\partial H}{\partial X}\right)^2 \left[\frac{\partial U}{\partial Z} + \delta^2 \frac{\partial W}{\partial X} - B\frac{\partial c}{\partial X}\frac{\partial c}{\partial Z}\right] + \frac{\partial H}{\partial X}\left[2\delta^2 \frac{\partial W}{\partial Z} - B\left(\frac{\partial c}{\partial Z}\right)^2\right] = 0, \quad (2.15)
\end{aligned}
$$

where Marangoni effects are neglected.

The kinematic boundary condition is:

$$W = \pm\left(\frac{\partial H}{\partial T} + U\frac{\partial H}{\partial X}\right). \quad (2.16)$$

The boundary conditions for the concentration at $Z = \pm H$, i.e. $\nabla\hat{n}.\nabla c = \hat{n}.\nabla\nabla^2 c = 0$ are

$$-\delta^2 H_X c_X \pm c_Z = 0 \quad (2.17)$$

$$\text{and} \quad -\delta^4 H_X c_{XXX} - \delta^2 H_X c_{ZZX} \pm \delta^2 c_{ZXX} \pm c_{ZZZ} = 0. \quad (2.18)$$

At $Z = 0$, the conditions imposed are:

$$U_Z = 0; \quad (2.19a)$$

$$W = 0; \quad (2.19b)$$

$$c_Z = 0; \quad (2.19c)$$

$$\text{and} \quad c_{ZZZ} = 0. \quad (2.19d)$$

2.3 Derivation of Navier-Stokes-Cahn-Hilliard equations for a free-film

Expanding the variables P, U, W and c in series as $P = P_0 + \delta P_1 + \delta^2 P_2 + \ldots, U = U_0 + \delta U_1 + \delta^2 U_2 + \ldots, W = W_0 + \delta W_1 + \delta^2 W_2 + \ldots$ and $c = c_0 + \delta c_1 + \delta^2 c_2 + \ldots$ respectively, leads to the following problems in increasing orders of δ.

Since the scaling chosen for the interphase boundary thickness can vary, the gas-liquid interface conditions are first given. At $Z = \pm H$, the $O(1)$ conditions are:

$$c_{0Z} = c_{0ZZZ} = 0; \quad (2.20)$$

at $O(\delta)$,

$$c_{1Z} = c_{1ZZZ} = 0; \tag{2.21}$$

at $O(\delta^2)$,

$$\frac{\partial c_2}{\partial Z} = \pm H_X \frac{\partial c_0}{\partial X} \tag{2.22a}$$

$$\text{and} \quad c_{2ZZZ} = 0. \tag{2.22b}$$

Finally at $O(\delta^3)$,

$$\frac{\partial c_3}{\partial Z} = \pm H_X \frac{\partial c_1}{\partial X} \tag{2.23a}$$

$$\text{and} \quad c_{3ZZZ} = 0. \tag{2.23b}$$

At $Z = 0$, the $O(1)$ conditions are:

$$c_{0Z} = c_{0ZZZ} = 0; \tag{2.24}$$

at $O(\delta)$,

$$c_{1Z} = c_{1ZZZ} = 0; \tag{2.25}$$

at $O(\delta^2)$,

$$c_{2Z} = c_{2ZZZ} = 0; \tag{2.26}$$

and at $O(\delta^3)$,

$$c_{3Z} = c_{3ZZZ} = 0. \tag{2.27}$$

2.4 Case 1

The interphase boundary thickness is governed by the parameter $\sqrt{\gamma}$ which is included in the definition of $C_n = \dfrac{\sqrt{\gamma}}{h_0}$. Therefore, the scale for the interphase boundary thickness can be larger or smaller than the film thickness and we will examine both cases. In thin-film research involving lubrication theory, investigators have typically assumed $\sqrt{\gamma} >> h_0$, rendering the compositional profile strictly unidirectional in the longitudinal coordinate X. As will be shown below, the layering of phases within the free-film requires the opposite limit, i.e. $\sqrt{\gamma} << h_0$.

In this section, the evolution equations are derived for the physical situation where the thickness of the interphase boundary is much less than the thickness of the film, i.e. $\sqrt{\gamma} << h_0$. Setting $(\delta C_n)^2 \sim O(\delta^4)$ gives $C_n \sim O(\delta)$. Let $C_n = \delta \tilde{C_n}$, where $\tilde{C_n} \sim O(1)$. Then $B = \dfrac{\beta\gamma}{\nu D} = \dfrac{\beta C_n^2 h_0^2}{\nu D} = \delta^2 \left[\dfrac{\beta \tilde{C_n^2} h_0^2}{\nu D}\right]$. Now assume $\beta = \dfrac{\hat{\beta}}{\delta^2}$, where $\hat{\beta} \sim O(1)$, then β is very large. This scaling is necessary for the concentration to play a role in the momentum equations. This makes $B \sim O(1)$.

At $O(1)$, the Cahn-Hilliard concentration equation becomes

$$\frac{\partial^2}{\partial Z^2}(c_0^3 - c_0) = 0. \tag{2.28}$$

Integrating in Z and using (2.20) gives

$$c_0 = \pm\sqrt{\frac{1}{3}} \quad \text{or} \quad \frac{\partial c_0}{\partial Z} = 0. \tag{2.29}$$

Similarly at $O(\delta)$,

$$\frac{\partial^2 c_1}{\partial Z^2} = 0; \tag{2.30a}$$

$$\frac{\partial c_1}{\partial Z} = 0; \tag{2.30b}$$

and at $O(\delta^2)$,

$$\frac{\partial c_0}{\partial T} + U_0 \frac{\partial c_0}{\partial X} = (3c_0^2 - 1)\left[\frac{\partial^2 c_0}{\partial X^2} + \frac{\partial^2 c_2}{\partial Z^2}\right]. \tag{2.31}$$

Using these results, the equations of motion at $O(1)$ are:

$$-\frac{\partial P_0}{\partial X} + \frac{\partial^2 U_0}{\partial Z^2} = 0; \tag{2.32a}$$

$$\frac{\partial P_0}{\partial Z} = 0; \tag{2.32b}$$

at $O(\delta)$,

$$-\frac{\partial P_1}{\partial X} + \frac{\partial^2 U_1}{\partial Z^2} = 0; \tag{2.33a}$$

$$\frac{\partial P_1}{\partial Z} = 0; \tag{2.33b}$$

and finally at $O(\delta^2)$,

$$Re\left[\frac{\partial U_0}{\partial T}+U_0\frac{\partial U_0}{\partial X}+W_0\frac{\partial U_0}{\partial Z}\right]=-\frac{\partial P_2}{\partial X}-\frac{\partial \Phi}{\partial X}+\frac{\partial^2 U_0}{\partial X^2}+\frac{\partial^2 U_2}{\partial Z^2}-B\frac{\partial c_0}{\partial X}\frac{\partial^2 c_0}{\partial X^2}-B\frac{\partial c_0}{\partial X}\frac{\partial^2 c_2}{\partial Z^2};\tag{2.34a}$$

$$\text{and}\quad \frac{\partial P_2}{\partial Z}=\frac{\partial^2 W_0}{\partial Z^2}\tag{2.34b}$$

The continuity equation at $O(1)$,

$$\frac{\partial U_0}{\partial X}+\frac{\partial W_0}{\partial Z}=0;\tag{2.35}$$

at $O(\delta)$,

$$\frac{\partial U_1}{\partial X}+\frac{\partial W_1}{\partial Z}=0;\tag{2.36}$$

at $O(\delta^2)$,

$$\frac{\partial U_2}{\partial X}+\frac{\partial W_2}{\partial Z}=0;\tag{2.37}$$

The gas-liquid interfacial conditions at $Z=\pm H$ at $O(1)$ are:

$$P_0=0;\tag{2.38a}$$

$$\frac{\partial U_0}{\partial Z}=0;\tag{2.38b}$$

$$W_0=\pm\left(\frac{\partial H}{\partial T}+U_0\frac{\partial H}{\partial X}\right);\tag{2.38c}$$

at $O(\delta)$,

$$P_1=0;\tag{2.39a}$$

$$\frac{\partial U_1}{\partial Z}=0;\tag{2.39b}$$

$$W_1=\pm U_1\frac{\partial H}{\partial X};\tag{2.39c}$$

and at $O(\delta^2)$,

$$-P_2\mp 2\frac{\partial H}{\partial X}\frac{\partial U_0}{\partial Z}+2\frac{\partial W_0}{\partial Z}=\tilde{Ca}^{-1}H_{XX};\tag{2.40a}$$

$$-2\frac{\partial H}{\partial X}\left(\frac{\partial U_0}{\partial X}-\frac{\partial W_0}{\partial Z}\right)\pm\frac{\partial U_2}{\partial Z}\pm\frac{\partial W_0}{\partial X}\mp B\frac{\partial c_0}{\partial X}\frac{\partial c_2}{\partial Z}=0;\tag{2.40b}$$

$$W_2=\pm U_2\frac{\partial H}{\partial X}.\tag{2.40c}$$

Finally at $Z = 0$, the conditions at $O(1)$ are:

$$U_{0Z} = W_0 = 0; \tag{2.41}$$

at $O(\delta)$,

$$U_{1Z} = W_1 = 0; \tag{2.42}$$

and at $O(\delta^2)$,

$$U_{2Z} = W_2 = 0. \tag{2.43}$$

The system of equations is solved as follows. From (2.32b), it is implied that $P_0(X,T)$. Integrating (2.32a) in Z gives $\left(\frac{\partial P_0}{\partial X}\right) Z = \frac{\partial U_0}{\partial Z} + f_1(X)$, and from (2.41), $f_1(X) = 0$. (2.38b) requires that in order for $\frac{\partial U_0}{\partial Z}$ to vanish at $Z = H$, then $\frac{\partial P_0}{\partial Z} = 0$ meaning that $P_0 = constant$. Furthermore, integration of $\frac{\partial U_0}{\partial Z} = 0$ implies that $U_0(X,T)$ is not a function of Z. $U_0(X,T)$ cannot be determined at $O(1)$ and so it is necessary to proceed to the next order in δ for its solution. Meanwhile, $W_{0Z} = -U_X$ so that $W_0 = -U_{0X}Z + f_2(X)$. But from (2.41), $f_2(X) = 0$.

At $O(\delta)$, it can be shown from (2.32a) and (2.33a) that $U_1(X,T)$ and that W_1 is linear in Z so that the contributions at $O(1)$ and $O(\delta)$ can be combined for example $P_0 + \delta P_1 = P_G$, and we can move on to $O(\delta^2)$. At $O(\delta^2)$, integrating (2.34b) in Z so that $P_2 = \frac{\partial W_0}{\partial Z} + f_3(X)$, defining a reduced pressure $P_2^* = P_2 - W_{0Z} + \Phi$ and using (2.35) and (2.38b), the boundary conditions at $Z = H$ become

$$-P_2^* + \Phi - U_{0X} = \tilde{Ca}^{-1} H_{XX} \tag{2.44}$$

$$4H_X U_{0X} + H U_{0XX} + B H_X \left(\frac{\partial c_0}{\partial X}\right)^2 = \frac{\partial U_2}{\partial Z} \tag{2.45}$$

Integrating the continuity equation (2.35) from $Z = 0$ to H using Leibnitz integral rule, $\frac{\partial}{\partial X}\int_0^H U_0 dZ + H_T = 0$ gives

$$\boxed{H_T + (U_0 H)_X = 0} \tag{2.46}$$

Also, from the continuity equation, $\frac{\partial U_0}{\partial X} Z + W_0$. On differentiating with respect to X,

$$W_{0X} = -U_{0XX} Z \tag{2.47}$$

and evaluating at $Z = H$, then

$$W_{0X} = -U_{0XX}H. \tag{2.48}$$

Substituting these expressions into (2.34a) gives

$$Re[U_{0T} + U_0U_{0X}] = -P_{2X}^* + 2U_{0XX} + U_{2ZZ} - B\frac{\partial c_0}{\partial X}\left[2\frac{\partial^2 c_0}{\partial X^2} + \frac{\partial^2 c_2}{\partial Z^2}\right]. \tag{2.49}$$

Integrating (2.49) in Z gives

$$ReZ[U_{0T} + U_0U_{0X}] = [-P_{2X}^* + 2U_{0XX}]Z + U_{2Z} - B\frac{\partial c_0}{\partial X}\left[2Z\frac{\partial^2 c_0}{\partial X^2} + \frac{\partial c_2}{\partial Z}\right] + f_4(X). \tag{2.50}$$

From (2.43), it is found that $f_4(X) = 0$, and from (2.44), (2.45) and (2.48),

$$f_4(X) = ReH[U_{0T}+U_0U_{0X}]-H[-\Phi_X+U_{0XX}+\tilde{Ca}^{-1}H_{XXX}+2U_{0XX}]-4H_XU_{0X}-HU_{0XX} - BH_X\left(\frac{\partial c_0}{\partial X}\right)^2 + B\frac{\partial c_0}{\partial X}\left[2\frac{\partial^2 c_0}{\partial X^2}H + H_X\frac{\partial c_0}{\partial X}\right].$$

The constant of integration determined at $Z = 0$ & $Z = H$ should be equal and on solving, we get

$$\boxed{ReH[U_{0T} + U_0U_{0X}] + H\left[\Phi_X - \tilde{Ca}^{-1}H_{XXX} - 2B\frac{\partial c_0}{\partial X}\frac{\partial^2 c_0}{\partial X^2}\right] = 4[HU_{0X}]_X} \tag{2.51}$$

In addition, integrating (2.31) in Z gives

$$\frac{\partial c_0}{\partial T}Z + U_0\frac{\partial c_0}{\partial X}Z = (3c_0^2 - 1)\left[\frac{\partial^2 c_0}{\partial X^2}Z + \frac{\partial c_2}{\partial Z}\right] + f_5(X)$$

From (2.22a),

$$f_5(X) = \frac{\partial c_0}{\partial T}H + U_0\frac{\partial c_0}{\partial X}H - (3c_0^2 - 1)\left[\frac{\partial^2 c_0}{\partial X^2}H + H_X\frac{\partial c_0}{\partial X}\right]$$

while from (2.43), $f_5(X) = 0$. Thus,

$$\boxed{H\left[\frac{\partial c_0}{\partial T} + U_0\frac{\partial c_0}{\partial X}\right] = (3c_0^2 - 1)\left[H\frac{\partial c_0}{\partial X}\right]_X} \tag{2.52}$$

The eqns. (2.46), (2.51) and (2.52) determine the evolution of the free-film. If β is chosen to be of higher order than $O(1)$ in δ, then B does not appear in the final equations. This means that composition does not affect the flow in (2.51) (although flow does affect species transport in (2.52)).

2.4.1 Linear stability analysis

Eqns. (2.46), (2.51) and (2.52) admit a solution in which the concentration c_0 is constant, U_0 is constant and H is uniform. We test the base state for its stability with respect to infinitesimally small perturbations. For a uniformly flat free-film, normal modes are used so that $c_0 = c^0 + \bar{c}\ exp(st + ikx), H = H^0 + \bar{H}\ exp(st + ikx)$, and $U_0 = U^0 + \bar{U}\ exp(st + ikx)$. Linearizing (2.46), (2.51) and (2.52) in the perturbation amplitudes $\bar{c}$, $\bar{U}$ and $\bar{H}$ gives

$$\bar{H}(s + U^0 ik) + \bar{U}(H^0 ik) = 0; \tag{2.53a}$$

$$\bar{U}(ReH^0 s + ReH^0 U^0 ik + 4H^0 k^2) + \bar{H}\left(-\frac{3\bar{A}}{H^{0^3}} ik + \tilde{Ca}^{-1} H^0 k^3 i\right) = 0; \tag{2.53b}$$

$$\text{and} \quad \bar{c}(s + U^0 ik + 3c^{0^2} k^2 - k^2) = 0 \tag{2.53c}$$

respectively, where $\bar{A}$ is defined such that $\Phi = \dfrac{\bar{A}}{H^3}$. Setting $H^0 = 1$ and $U^0 = 0$, we get the characteristic equation

$$(s + 3c^{0^2} k^2 - k^2)[Res^2 + 4k^2 s - 3\bar{A}k^2 + \tilde{Ca}^{-1} k^4] = 0 \tag{2.54}$$

For the above to vanish, either bracketed term can be equal to 0. Thus, $s + 3c^{0^2} k^2 - k^2 = 0$ represents a compositional (diffusional) mode and if $(3c^{0^2} - 1)k^2 < 0$, then $s > 0$, so that there is instability. This means that $(3c^{0^2} - 1) < 0$ or $|c^0| < \dfrac{1}{\sqrt{3}}$.

With the scaling that has been used, i.e. where the phases $c = +1$ or -1, the compositions $\pm\sqrt{\dfrac{1}{3}}$ are the boundaries of the spinodal region within which there is spontaneous separation of phases *via* spinodal decomposition(no nucleation). The other expression from the characteristic equation gives the same condition for instability given in Erneux and Davis[7], i.e. if $Re = 0$,

$$s = \frac{3\bar{A}}{4} - \frac{\tilde{Ca}^{-1} k^2}{4} \tag{2.55}$$

Eqn. (2.55) shows that the free-film is *unstable* because of van der Waals forces (because $\bar{A} > 0$), but the capillary forces stabilize the film. It can also be seen from (2.54) that the 'back reaction' term with the dimensionless coefficient B (which feeds the effects of concentration gradients into the flow equations) does not play any role in affecting the stability of the free-film, which is expected because these are non-linear terms.

2.5 Case 2

Here, the interphase boundary thickness is assumed to be larger than the film thickness. The scaling is similar to that used by Naraigh and Thiffeault[16] for the case of a thin-film (i.e. liquid layer on a substrate). Here, $\delta\frac{\sqrt{\gamma}}{h_0} = \delta C_n = \tilde{C_n}$, where $\tilde{C_n} \sim O(1)$. The rest of the parameters maintain the same scaling as in the previous section.

The concentration equation is now given by:

$$\delta^2\left[\frac{\partial c}{\partial T} + U\frac{\partial c}{\partial X} + W\frac{\partial c}{\partial Z}\right] = \delta^2\frac{\partial^2}{\partial X^2}(c^3 - c) + \frac{\partial^2}{\partial Z^2}(c^3 - c) - \delta^2{\tilde{C_n}}^2\frac{\partial^4 c}{\partial X^4} - \frac{{\tilde{C_n}}^2}{\delta^2}\frac{\partial^4 c}{\partial Z^4} - 2{\tilde{C_n}}^2\frac{\partial^2}{\partial X^2}\frac{\partial^2 c}{\partial Z^2} \quad (2.56)$$

The rescaled concentration equation expanded at increasing orders in δ becomes:

at $O(\frac{1}{\delta^2})$,

$$\frac{\partial^4 c_0}{\partial Z^4} = 0; \quad (2.57)$$

at $O(\frac{1}{\delta})$,

$$\frac{\partial^4 c_1}{\partial Z^4} = 0; \quad (2.58)$$

at $O(1)$,

$$\frac{\partial^4 c_2}{\partial Z^4} = 0; \quad (2.59)$$

at $O(\delta)$,

$$\frac{\partial^4 c_3}{\partial Z^4} = 0; \quad (2.60)$$

and at $O(\delta^2)$,

$$\frac{\partial c_0}{\partial T} + U_0\frac{\partial c_0}{\partial X} = \frac{\partial^2}{\partial X^2}(c_0^3 - c_0) + (3c_0^2 - 1)\frac{H_X}{H}\frac{\partial c_0}{\partial X} - {\tilde{C_n}}^2\frac{\partial^4 c_0}{\partial X^4} - 2{\tilde{C_n}}^2\frac{\partial^2}{\partial X^2}\frac{H_X}{H}\frac{\partial c_0}{\partial X} - {\tilde{C_n}}^2\frac{\partial^4 c_4}{\partial Z^4}. \quad (2.61)$$

Integrating (2.57) and (2.58) using (2.24) and(2.25) gives $\frac{\partial c_0}{\partial Z} = \frac{\partial c_1}{\partial Z} = 0$. Integration of (2.59) using (2.26) and (2.22a) gives

$$\text{at Z} = \text{H}, \quad \frac{\partial c_2}{\partial Z} = Z\frac{H_X}{H}\frac{\partial c_0}{\partial X} \quad \& \quad \frac{\partial^2 c_2}{\partial Z^2} = \frac{H_X}{H}\frac{\partial c_0}{\partial X} \; \forall \; Z \; \epsilon[-H, H], \quad (2.62)$$

and integration of (2.60) using (2.27) and (2.23a) gives

$$\text{at Z} = \text{H}, \quad \frac{\partial c_3}{\partial Z} = Z\frac{H_X}{H}\frac{\partial c_1}{\partial X} \quad \& \quad \frac{\partial^2 c_3}{\partial Z^2} = \frac{H_X}{H}\frac{\partial c_1}{\partial X} \; \forall \; Z \; \epsilon[-H, H]. \tag{2.63}$$

The boundary conditions for concentration remain the same as in the previous section. Using (2.62), a couple of added gas-liquid interface conditions from $O(\delta^4)$ are:
at $Z = \pm H$,

$$\frac{\partial c_4}{\partial Z} = \pm H_X \frac{\partial c_2}{\partial X}; \tag{2.64a}$$

$$\text{and} \quad \frac{\partial^3 c_4}{\partial Z^3} = \pm H_X \frac{\partial^3 c_0}{\partial X^3} \pm H_X \frac{\partial}{\partial X}\left(\frac{H_X}{H}\frac{\partial c_0}{\partial X}\right) - H\frac{\partial^2}{\partial X^2}\left(\frac{H_X}{H}\frac{\partial c_0}{\partial x}\right). \tag{2.64b}$$

Integrating (2.61) from $Z = 0$ to H, and upon solving gives the rescaled Cahn-Hilliard equation

$$\boxed{H\left[\frac{\partial c_0}{\partial T} + U_0\frac{\partial c_0}{\partial X}\right] = \left[H\frac{\partial \psi}{\partial X}\right]_X}, \tag{2.65}$$

where $\psi = c_0^3 - c_0 - \dfrac{\tilde{C_n}^2}{H}\dfrac{\partial}{\partial X}\left(H\dfrac{\partial c_0}{\partial X}\right)$. In this case, the eqns. (2.46), (2.51) and (2.65) determine the evolution of the free-film.

2.5.1 Linear stability analysis

Using normal modes and a procedure similar to that used in the previous case, eqns. (2.46), (2.51) and (2.65) are linearized about $H^0 = 1$ and $U^0 = 0$, the characteristic equation is determined to be

$$(s + 3c_0^2k^2 - k^2 + \tilde{C_n}^2k^4)[Res^2 + 4k^2s - 3\bar{A}k^2 + \tilde{C}a^{-1}k^4] = 0 \tag{2.66}$$

The above equation is very similar to the characteristic equation from the previous section and same explanation for the conditions of instability hold for this case as well. Also, as can be seen from (2.66), the 'back reaction' term with the dimensionless coefficient B does not play any role in affecting the stability of the free-film in this case either.

2.6 Layered phases in films

In this section, a profile of the interphase boundary is determined for the case where the thickness of the interphase boundary is much less than the thickness of the free-film, i.e.

$C_n = \delta\tilde{C_n}$, where $\tilde{C_n} \sim O(1)$. In this case, c can take the values $+1$ or -1 throughout the entire phase indicating either α or β phase. It is also possible to have regions of $+1$ and -1 that are separated by narrow interfacial regions. We seek to determine the compositional profile in a film with two layered phases.

Within the interfacial region, the thickness needs to be scaled differently because the concentration gradient there becomes large. Define the inner variable $Z^* = \dfrac{Z}{Z_0}$, where the outer variable $Z\epsilon[-H, H]$ and define c^* to represent the concentration in this region. Under steady-state conditions with no flow, the concentration equation at the lowest order $\dfrac{\partial^2}{\partial Z^2}(c^3 - c) = \delta^2 \tilde{C_n}^2 \dfrac{\partial^4 c}{\partial Z^4}$ is transformed to

$$\frac{1}{Z_0^2}\frac{\partial^2}{\partial Z^{*2}}(c^{*3} - c^*) = \delta^2 \frac{\tilde{C_n}^2}{Z_0^4}\frac{\partial^4 c^*}{\partial Z^{*4}}. \tag{2.67}$$

Terms balance by setting Z_0 equal to δ so that $Z = \delta Z^*$. Assuming the phase separated components to have compositions $+1$ at the top layer and -1 for the bottom layer, the boundary conditions ${c^*}_Z = {c^*}_{ZZZ} = 0$ as $Z \to \pm\bar{H}$ now become

$${c^*}_{Z^*} = {c^*}_{Z^*Z^*Z^*} = 0 \text{ as } Z^* \to \pm\infty \tag{2.68a}$$

$$\text{And as } Z^* \to \pm\infty, \text{ the limiting composition } c^* \to \pm 1 \tag{2.68b}$$

Eqn. (2.67) becomes $\dfrac{\partial^2}{\partial Z^{*2}}(c^{*3} - c^*) = \tilde{C_n}^2 \dfrac{\partial^4 c^*}{\partial Z^{*4}}$, which may be integrated to give

$$\frac{\partial}{\partial Z^*}(c^{*3} - c^*) = \tilde{C_n}^2 \frac{\partial^3 c^*}{\partial Z^{*3}} + A_1.$$

From (2.68a), $A_1 = 0$.

Integrating again,

$$(c^{*3} - c^*) = \tilde{C_n}^2 \frac{\partial^2 c^*}{\partial Z^{*2}} + A_2 \tag{2.69}$$

Multiplying (2.69) by $\left(\dfrac{\partial c^*}{\partial Z^*}\right)$ and integrating in Z^* gives

$$\frac{\tilde{C_n}^2}{2}\left(\frac{\partial c^*}{\partial Z^*}\right)^2 = \frac{c^{*4}}{4} - \frac{c^{*2}}{2} - A_2 c^* + A_3$$

Using (2.68a) and (2.68b), $A_2 = 0$ & $A_3 = 1/4$. Taking square root on both sides, separating the variables and integrating, the profile for the interphase boundary is found to be

$$\boxed{c^* = tanh\left[\frac{Z^* + A_4}{\sqrt{2}\tilde{C_n}}\right]}, \tag{2.70}$$

where A_4 is a constant of integration, representing a translation of the interphase location.

2.6.1 Matching inner and outer solutions

Eqn. (2.70) represents the inner solution and needs to be matched to the outer solution, $c = \pm 1$. An intermediate variable technique will be used for matching the inner and outer solutions[27] of the free-film, the inner solution being the profile of the interphase boundary while the outer solution is that the top and bottom layers have the composition ± 1. Define a function $\eta(\delta)$ that remains bounded as $\delta \to 0$ (where $0 << \delta << \eta << 1$) and an intermediate space variable $Z_\eta = \dfrac{Z}{\eta}$. Using this, the space variable for the outer problem is given by $Z = \eta Z_\eta$. At the outer limits of the interphase boundary, $c = \pm 1$ as $\delta \to 0$, and the space variable for the inner problem is given by $Z^* = \dfrac{\eta Z_\eta}{\delta}$.

Now, keeping Z_η fixed, the matching condition for the inner and outer regions at the upper limit is given by

$$\lim_{\delta \to 0} [c^*(Z^*) - c(Z)] = 0.$$

Writing in terms of the intermediate variable gives

$$\lim_{\delta \to 0} \left[c^*\left(\frac{\eta Z_\eta}{\delta}\right) - c(\eta Z_\eta)\right] = 0$$

and from (2.70),

$$\lim_{\delta \to 0} \left\{tanh\left[\frac{1}{\sqrt{2}\tilde{C_n}}\left(\frac{\eta Z_n}{\delta}\right)\right] - c(\eta Z_\eta)\right\} = 0,$$

which is obeyed automatically. Similarly, the matching condition for the inner and outer regions at the lower limit is given by

$$\lim_{\delta \to 0} \left[c^*\left(\frac{\eta Z_\eta}{\delta}\right) - c(\eta Z_\eta)\right] = 0$$

and from (2.70),

$$\lim_{\delta \to 0} \left\{tanh\left[\frac{1}{\sqrt{2}\tilde{C_n}}\left(\frac{\eta Z_n}{\delta}\right)\right] - c(\eta Z_\eta)\right\} = 0$$

which is also satisfied. The composite solution is achieved by adding the inner and outer solutions and subtracting the matching terms as follows,

$$c = tanh\left[\frac{Z^* - A_4}{\sqrt{2}\tilde{C}_n}\right] + 1 - 1 - 1 + 1$$

and thus

$$\boxed{c = tanh\left[\frac{Z^* - A_4}{\sqrt{2}\tilde{C}_n}\right]},$$

where the constant A_4 may be set to 0 without any loss of generality.

In this case, the final matched solution describing the profile of the free-film happens to be the same as that of the solution for the interphase boundary.

2.7 Conclusion

In this chapter, the evolution equations for a free-film undergoing phase separation have been derived using the theoretical framework of the long-wave theory and extensional flow. A set of three equations that describe the evolution of the free-film have been derived for two cases, where the interphase boundary is assumed to be smaller and larger in thickness than the free-film. The phase separated fluid components are assumed to be density and viscosity matched and the equations include the van der Waals forces between the two free surfaces. On performing a linear stability analysis, the results from both cases show that there is instability due to compositional modulations leading to phase transformation within the film (Cahn-Hilliard mode[28, 29]). Also, a hydrodynamic instability may occur due to van der Waals forces (Erneux-Davis mode[7]). Except for the translational velocity U_0, the growth of these modes is uncoupled since the back reaction term only comes in through the non-linear terms.

This chapter also derives the profile of the interphase boundary for a binary liquid solution capable of phase separation by using a matched asymptotic analysis. This has been done for the case where the interphase boundary thickness is lesser than the film thickness. Such a configuration allows for a layered structure of the phases in the film. Equilibrium conditions have been studied, i.e. assuming a steady state and no-flow.

2.8 Future work

In the future, differences in density and viscosity for the phase separated components may be included in the derivation for the evolution equations. It is of interest to look at a system of phase separated fluids by including different Hamaker constants for the various fluid-fluid interactions. Future work should investigate the stability of the interphase boundary by inducing a flow into the system. A numerical analysis may also be done to study the non-linear coupling of flow on phase change.

Chapter 3

WETTING AT THE PHASE BOUNDARIES IN A FREE-FILM

3.1 One-dimensional case

3.1.1 Model

In this chapter, a free-film alloy is considered with an average initial composition c_{avg}. The geometry and the physical conditions are set as follows. The film extends from $x = 0$ to $x = L$. The limiting composition of the fluid at the phase boundaries at $x = 0$ and $x = L$ is a variable c_s and the free energy of the phase boundary interacting at the free surfaces is $\Phi(c_s)$. Using the expression given by Cahn and Hilliard for the free energy of a non-uniform system defined as $F = N_v \int_v \left[f_0(c) + K(\nabla c)^2 \right] dv$, where N_v is the number of molecules per unit volume, ∇c is the concentration gradient, f_0 is the free energy of a molecule in a homogeneous system of composition c and K is a positive constant[25], the excess free energy of unit area of surface is given by

$$\Delta F = 2\Phi(c_s) + \int_0^L \left[\Delta f + K \left(\frac{dc}{dx} \right)^2 \right] dx, \tag{3.1}$$

where $\Delta f = f(c) - f(c_{avg}) - (c - c_{avg}) \left(\frac{df}{dc} \right)_{c_{avg}}$ is the free energy needed to create a unit volume of uniform fluid composition c from a reservoir at composition c_{avg}, $K \left(\frac{dc}{dx} \right)^2$ is the contribution to the free energy due to the presence of a gradient. The $2\Phi(c_s)$ is to include the free energy contributions due to two identical free surfaces. Since the domain of the problem considered here is finite and no mass is lost from the liquid, a conservation of mass condition is imposed *viz.*,

$$\int_0^L (c - c_{avg}) dx = 0. \tag{3.2}$$

By finding the composition profile that minimizes the function

$$\psi = 2\Phi(c_s) + \int_0^L \left[\Delta f + K \left(\frac{dc}{dx} \right)^2 \right] dx + \lambda \int_0^L (c - c_{avg}) dx, \tag{3.3}$$

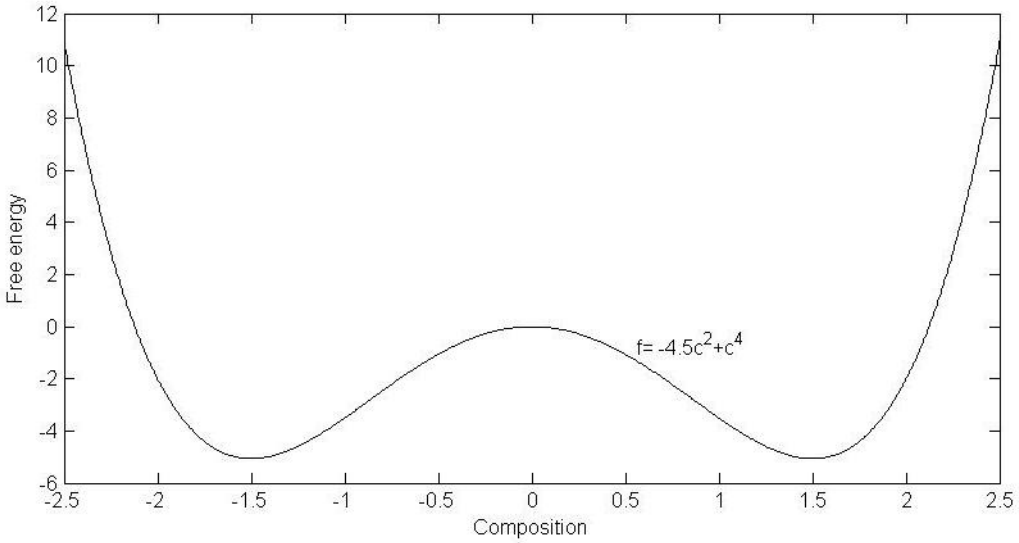

Figure 3.1: *Free energy vs. Composition* curve considered for the problem. The stable compositions for this profile are c=-1.5 and c=+1.5

where λ is the Lagrange multiplier, we can observe whether phases wet the film boundary or not. Cahn treated this problem for a semi-infinite system[18], whereas here we treat a finite system.

Using variational calculus, the condition

$$f' - \left(\frac{\partial f}{\partial c}\right)_{c_{avg}} - 2K\frac{\partial^2 c}{\partial x^2} + \lambda = 0 \tag{3.4}$$

subject to the boundary conditions at $x = 0$ and $x = L$,

$$\Phi' = 2K\left(\frac{\partial c}{\partial x}\right)_{x=0} \text{ and } \Phi' = 2K\left(\frac{\partial c}{\partial x}\right)_{x=L}, \tag{3.5}$$

respectively will minimize (3.1) subject to (3.2). This solution is carried out numerically.

3.1.2 Numerical method

The domain $x\epsilon[0, L]$ is divided into $N + 1$ nodes with equal spacing h. The unknowns are the concentrations at each of the nodes and λ (the Lagrange multiplier), i.e. $N + 2$ unknowns. The concentrations at the phase boundaries are $c_1 = c_s$ at $x = 0$ and $c_{N+1} = c_s$

at $x = L$. The contribution to the free energy at the free surfaces is assumed to be of the form $\Phi = \Phi_0 - \Phi_1 c_s + \frac{1}{2}\Phi_2 {c_s}^2$ so that we get the linear plot

$$-\Phi' = \Phi_1 - \Phi_2 c_s \tag{3.6}$$

for use in the boundary conditions (3.5), (see *de Gennes*[26]). Now, differentiating $\Delta f = f(c) - f(c_{avg}) - (c - c_{avg}) \left(\frac{\partial f}{\partial c}\right)_{c_{avg}}$ with respect to x, we get

$$\frac{\partial}{\partial x}(\Delta f) = \left[f' - \left(\frac{\partial f}{\partial c}\right)_{c_{avg}}\right] \frac{\partial c}{\partial x}. \tag{3.7}$$

Multiplying (3.4) by $\frac{\partial c}{\partial x}$ gives

$$\left[f' - \left(\frac{\partial f}{\partial c}\right)_{c_{avg}}\right] \frac{\partial c}{\partial x} - \left[K \left(\frac{\partial c}{\partial x}\right)^2\right]_x + \lambda \frac{\partial c}{\partial x} = 0, \tag{3.8}$$

and from (3.7) and (3.8),

$$\frac{\partial}{\partial x}(\Delta f) - \left[K \left(\frac{\partial c}{\partial x}\right)^2\right]_x + \lambda \frac{\partial c}{\partial x} = 0. \tag{3.9}$$

Integrating in x gives

$$\Delta f - K \left(\frac{\partial c}{\partial x}\right)^2 + \lambda c + const = 0. \tag{3.10}$$

If the thickness of the film is considerably larger than the region of wetting, the boundary conditions chose are $c \to c_{avg}$, $\frac{\partial c}{\partial x} \to 0$ and $\Delta f \to 0$, which are the same as would be used in an infinite system (i.e. a system of one interface). From these conditions, $const = -\lambda c$, thus

$$\Delta f = K \left(\frac{\partial c}{\partial x}\right)^2,$$
$$\text{or} \quad \frac{dc}{dx} = \pm \left(\frac{\Delta f}{K}\right)^{1/2}.$$

Plugging this into (3.5) and squaring both sides gives

$${\Phi'}^2 = 4K\Delta f(c_s), \text{ since } c = c_s \text{ at } x = 0 \text{ and } x = L. \tag{3.11}$$

From (3.6) and (3.11), the equations for the concentration at the boundaries are

$$\Phi_1^2 + \Phi_2^2 - 2\Phi_1\Phi_2 c_1 = 4K\left[(-ac_1^2 + bc_1^4) - (-a{c_{avg}}^2 + b{c_{avg}}^4)\right] \tag{3.12}$$

$$\text{and} \quad \Phi_1^2 + \Phi_2^2 - 2\Phi_1\Phi_2 c_{N+1} = 4K\left[(-ac_{N+1}^2 + bc_{N+1}^4) - (-a{c_{avg}}^2 + b{c_{avg}}^4)\right], \tag{3.13}$$

where subscripts denote the node. For the $N-1$ interior nodes, applying a central difference formula for the derivative of second-order gives

$$f'(c_n) - \left(\frac{\partial f}{\partial c}\right)_{c_{avg}} - 2K\left[\frac{c(n+1) - 2c(n) + c(n-1)}{h^2}\right] + \lambda = 0. \tag{3.14}$$

Using the trapezoidal rule for the conservation of mass gives

$$\frac{1}{2}h(c_1 + 2(c_2 + c_3 + \ldots + c_N) + c_{N+1} - 2Nc_{avg}) = 0. \tag{3.15}$$

Thus, there are $N+2$ unknowns and $N+2$ equations. Since there is a non-linear function in (3.14), an iterative method is needed to solve the system of equations. In this case, a damped newton method was used. All of the computations and the plots have been done in *MATLAB*.

3.1.3 Plots and analysis

The free energy of the free-film is assumed to be of the form $f = -ac^2 + bc^4$, where a and b are constants, thus having two stable energy minima compositions with an energy maxima at $c = 0$. Here, the constants are taken to be $a = 4.5$ and $b = 1$, such that the free-film is stable at compositions -1.5 and $+1.5$, as can be seen in Figure 3.1. For the first set of calculations, the size of the domain was set to $L = 100$ and by applying 2000 nodes in the interval $x\epsilon[0, 100]$.

For the first case, the initial average composition $c_{avg} = -1.5$, Φ' is assumed such that $\Phi_1 = 3$ and $\Phi_2 = 2$ in (3.12) and as shown in Figure (3.2)(a). The plots $(b), (c)$ and (d) are achieved by changing the value of Φ_1 to $4, 6$ and 7 respectively. The constant is chosen as $K = 2$.

The intersection at I gives the composition at the free surfaces for plots (a) and (b) and it can be seen that there is no wetting from the other phase since $c_s = -0.8$. In plot (c) however, the area between the curves intersecting at points II and III, is greater

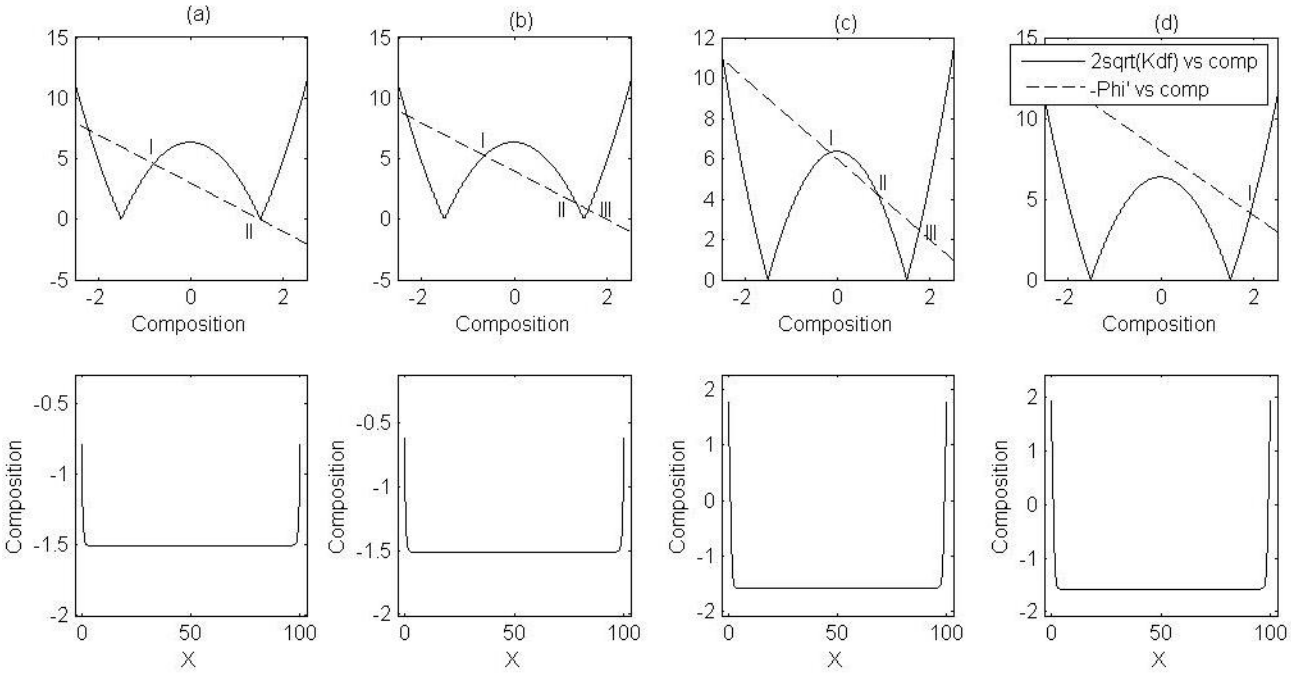

Figure 3.2: $2\sqrt{Kdf}$ and $-\Phi'$ *vs. Composition* and simultaneous composition profiles for a 1-D free-film with $c_{avg} = -1.5$. Cahn[18] used the upper figures to examine wetting in a semi-infinite system.

than the area between the curves between the points I and II. According to theory of Cahn, this renders the interfacial region unstable to the formation of a wetting phase. This configuration lowers the free energy of the system. Cahn's theory states that a first-order transition takes place when the area under the solid line and the dashed line between points I and II becomes less than the area between the dashed and solid line from points II and III. The wetting composition at the free surface is given by point III. In plot (d), there is still wetting, in which case, the wetting composition is given by point I.

For the next case, the initial average composition of the film is taken to be $c_{avg} = +1.5$ as seen in Figure 3.3. The rest of the parameters remain unchanged. In this case, it is seen that there is phase wetting at the gas-liquid interface in (a) and (b) as this results in a lower overall free energy of the system and the wetting composition is given by I. In (c) and (d), it can be seen that the unstable phase no longer wets the phase boundary and that a

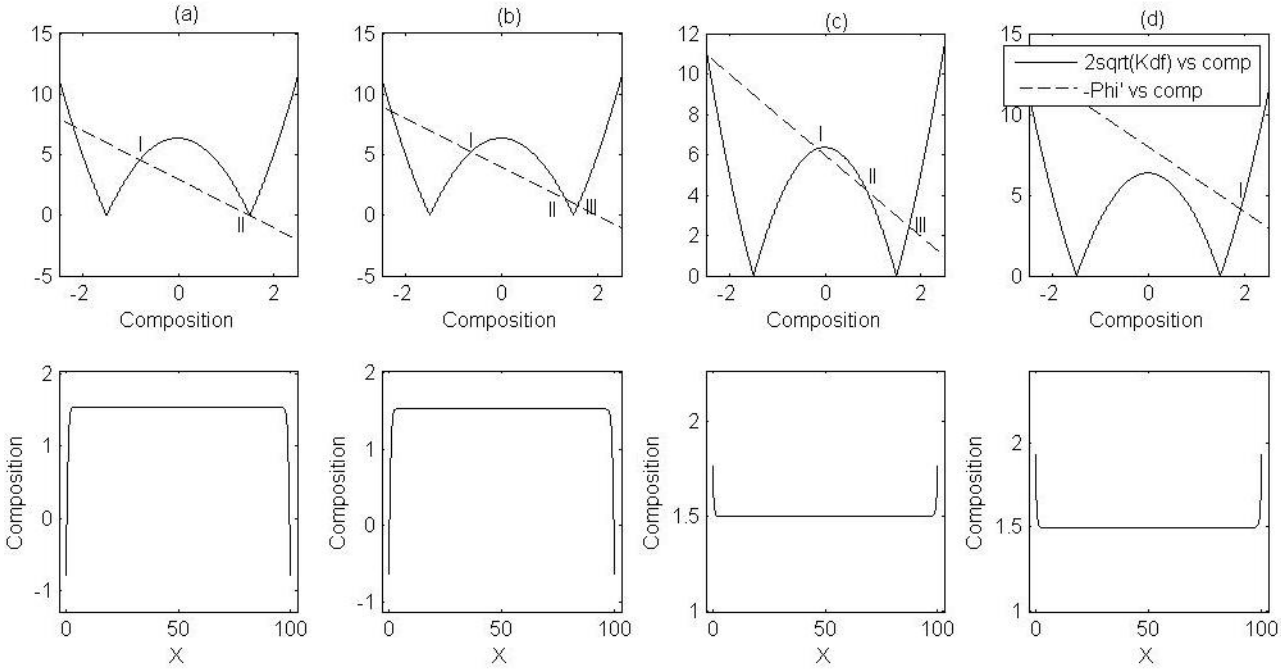

Figure 3.3: $2\sqrt{Kdf}$ and $-\Phi'$ *vs. Composition* and simultaneous composition profiles for a 1-D free-film with $c_{avg} = +1.5$

first-order transition takes place when the area under the curves between I and II is equal to the area under the curves between II and III. The composition at the free surfaces for these cases is given by III and I respectively.

3.2 Cylindrical geometry

3.2.1 Model

In this section, the wetting at the phase boundary is numerically simulated for a free-film having a cylindrical geometry. The geometry and the physical conditions are set up as follows. The model is derived for an axisymmetric case and thus the equations and plots are given for just the radius extending from $r = 0$ to $r = R$.

Using the expression given by Cahn and Hilliard for the free energy, the excess free

energy of unit area due to the surface is now given by

$$\Delta F = 2\pi R\Phi(c_s) + \int_0^R \left[\Delta f + K\left(\frac{\partial c}{\partial r}\right)^2\right] r dr \tag{3.16}$$

And the conservation of mass condition is

$$2\pi \int_0^R (c - c_{avg}) r dr \tag{3.17}$$

Now, it is necessary to find the composition profile that minimizes the function

$$\psi = \Delta F + \lambda 2\pi \int_0^R (c - c_{avg}) r dr \tag{3.18}$$

As in the previous section, using variational calculus, the minimization condition for this case is found to be

$$f' - \left(\frac{\partial f}{\partial c}\right)_{c_{avg}} - 2K\frac{\partial^2 c}{\partial r^2} - \frac{2K}{r}\frac{\partial c}{\partial r} + \lambda = 0 \tag{3.19}$$

And the boundary condition at $r = R$,

$$\Phi' = 2K\left(\frac{\partial c}{\partial r}\right)_{r=R} \tag{3.20}$$

Due to symmetry, we have the boundary condition at $r = 0$ as

$$\frac{\partial c}{\partial r} = 0 \tag{3.21}$$

3.2.2 Numerical solutions

The numerics are very similar to those used in the 1-D Cartesian case of the previous section. The domain is divided into $N + 1$ nodes with equal spacing 'h' in between representing $r\ \epsilon[0, R]$. The concentration at the phase boundary $r = R$ is $c_{N+1} = c_s$. The boundary condition for concentration is the same as (3.13). The boundary condition at r=0, i.e. (3.20) using a finite difference is

$$\frac{c_2 - c_1}{h} = 0 \tag{3.22}$$

For the $N-1$ interior nodes, using a central difference for the first and second-order derivatives,

$$f'(c_n) - \left(\frac{\partial f}{\partial c}\right)_{c_{avg}} - 2K\left[\frac{c(n+1) - 2c(n) + c(n-1)}{h^2}\right] - \frac{2K}{r_n}\left[\frac{c_{n+1} - c_{n-1}}{2h}\right] + \lambda = 0, \tag{3.23}$$

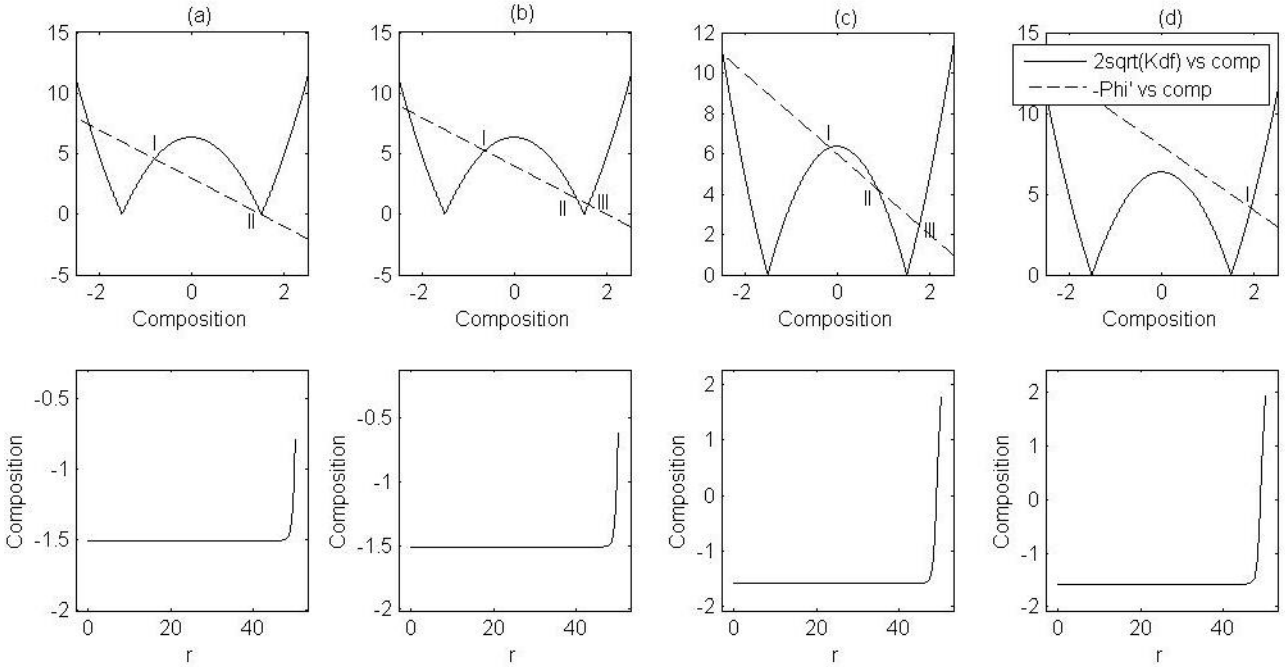

Figure 3.4: $2\sqrt{Kdf}$ and $-\Phi'$ *vs. Composition* and simultaneous composition profiles for an axisymmetric cylindrical free-film with $c_{avg} = -1.5$

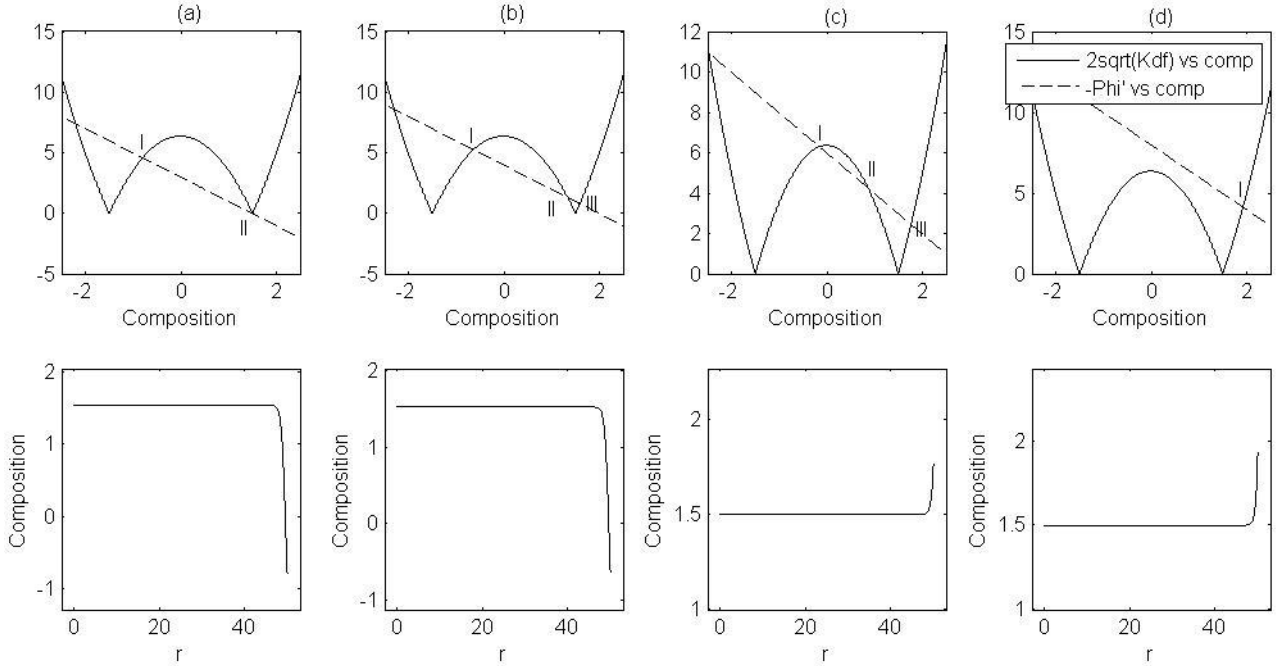

Figure 3.5: $2\sqrt{Kdf}$ and $-\Phi'$ *vs. Composition* and simultaneous composition profiles for an axisymmetric cylindrical free-film with $c_{avg} = +1.5$

where r_n is the radius evaluated at the n^{th} node.

The conservation of mass equation remains the same as before. The system of equations is solved using the same numerical methods described in the previous section and the plots for the various cases are plotted.

3.2.3 Plots

For the numerical simulations, the domain $r\epsilon[0, 50]$ was divided into 2000 intervals. All other parameters and initial conditions remain the same as in the previous section. The results for this geometry are very similar to the 1-D case and the previous explanations for the final composition profiles hold for this case as well. The two cases, one starting with an average initial composition of $c_{avg} = -1.5$ and the other starting with an average initial composition of $c_{avg} = +1.5$ were examined and the results are plotted in Figures 3.4 and 3.5 respectively.

3.3 The effect of film thickness

In this section, the composition profile of the free-film is examined while the thickness of the film is made thinner gradually. The equations used and assumptions are all the same as in the previous section. The boundary condition at the domain boundaries, however, need to be modified because the approximation given by (3.11) can no longer be used for these finite films, instead the general conditions (3.5) are required. From (3.5), using finite differences, the boundary conditions for the concentration, i.e. $c_1 = c_s$ at $x = 0$ and $x = L$ for the 1-D case and at $r = R$ for the cylindrical case are

$$c_1 = \frac{\Phi_1 h + 2Kc_2}{2K + h\Phi_2} \tag{3.24a}$$

$$c_{N+1} = \frac{\Phi_1 h + 2Kc_N}{2K + h\Phi_2} \tag{3.24b}$$

It is interesting to see how the concentration profile is affected by the thickness of the free-film, as shown for the case in which $\Phi_1 = 12$. For this case, the free-film with $c_{avg} = -1.5$ is wetted at the phase boundary by the unstable phase, whereas for the case

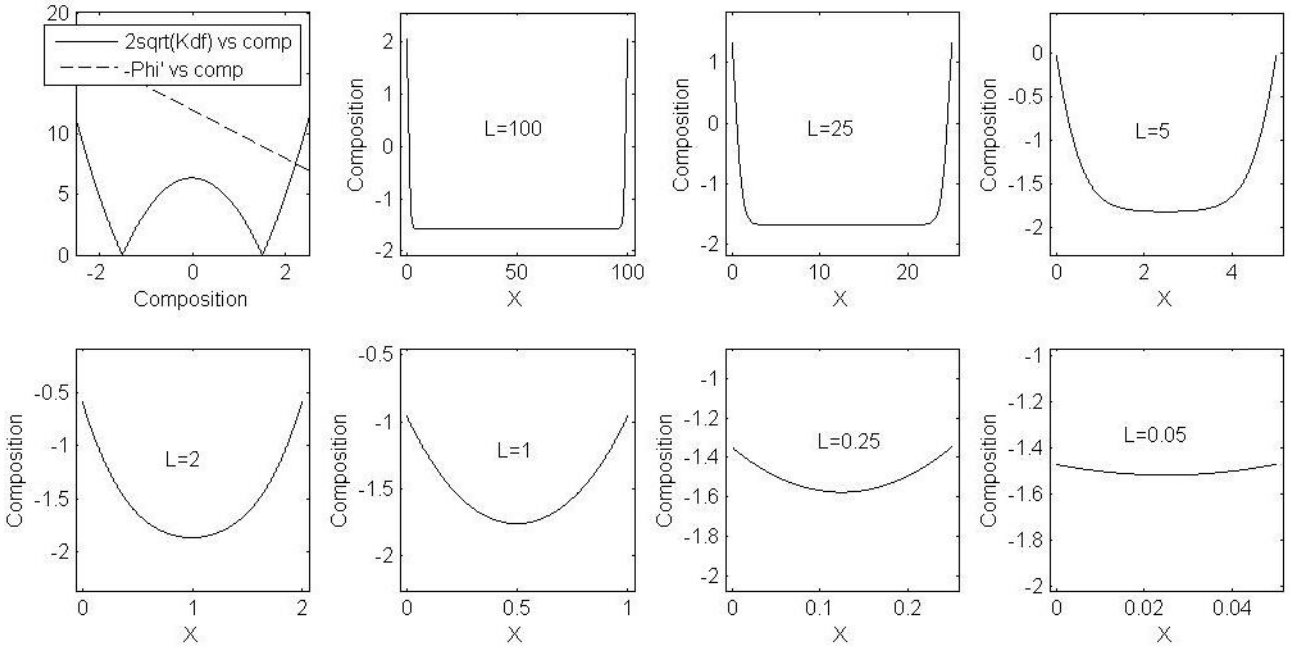

Figure 3.6: Composition profiles for a 1-D free-film with an initial average composition of $c_{avg} = -1.5$

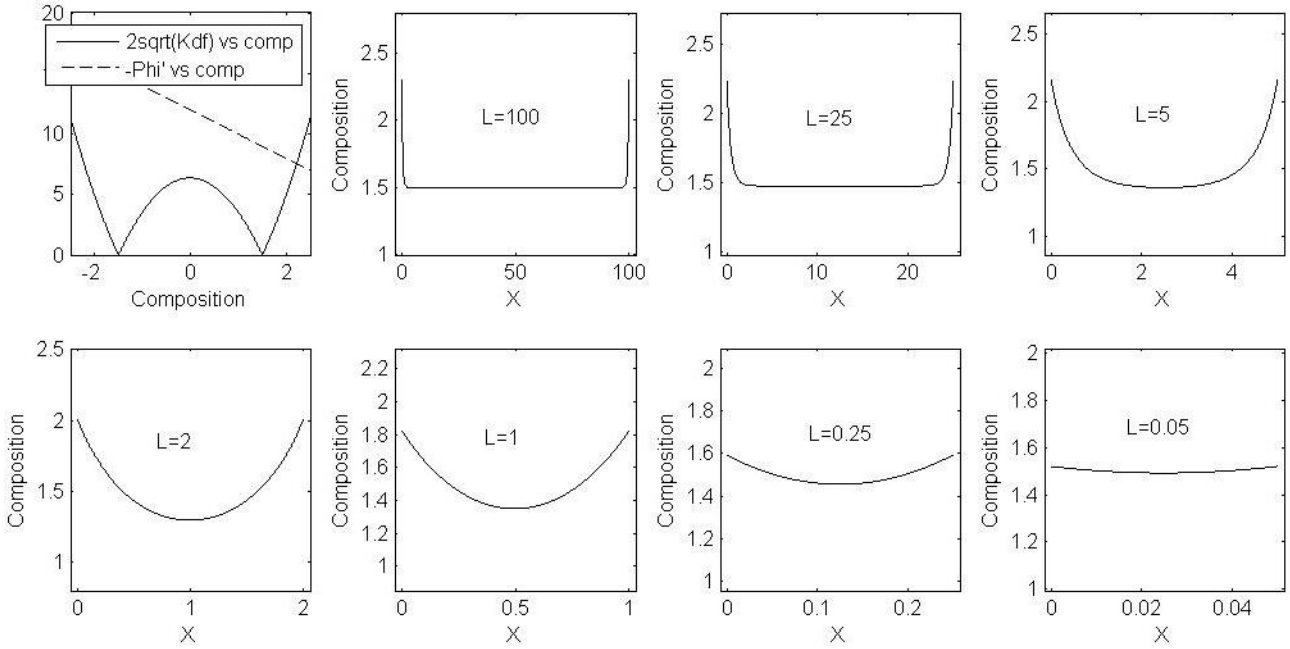

Figure 3.7: Composition profiles for a 1-D free-film with an initial average composition of $c_{avg} = +1.5$

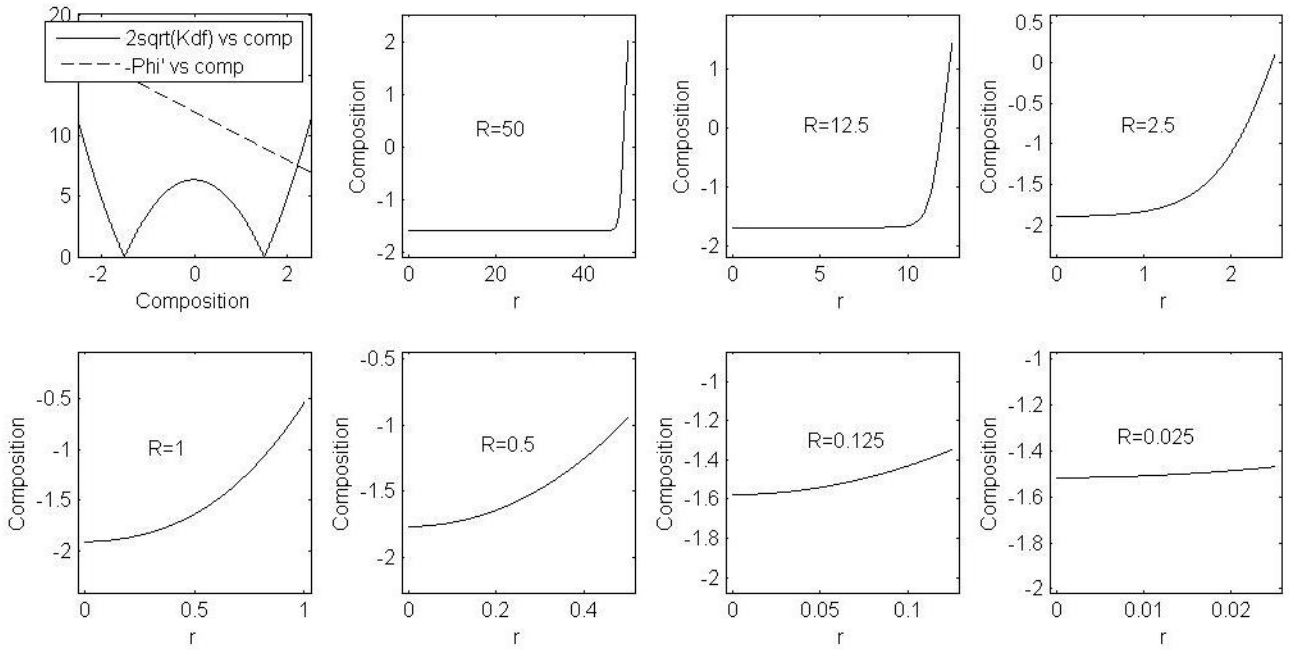

Figure 3.8: Composition profiles for an axisymmetric cylindrical free-film with an initial average composition of $c_{avg} = -1.5$

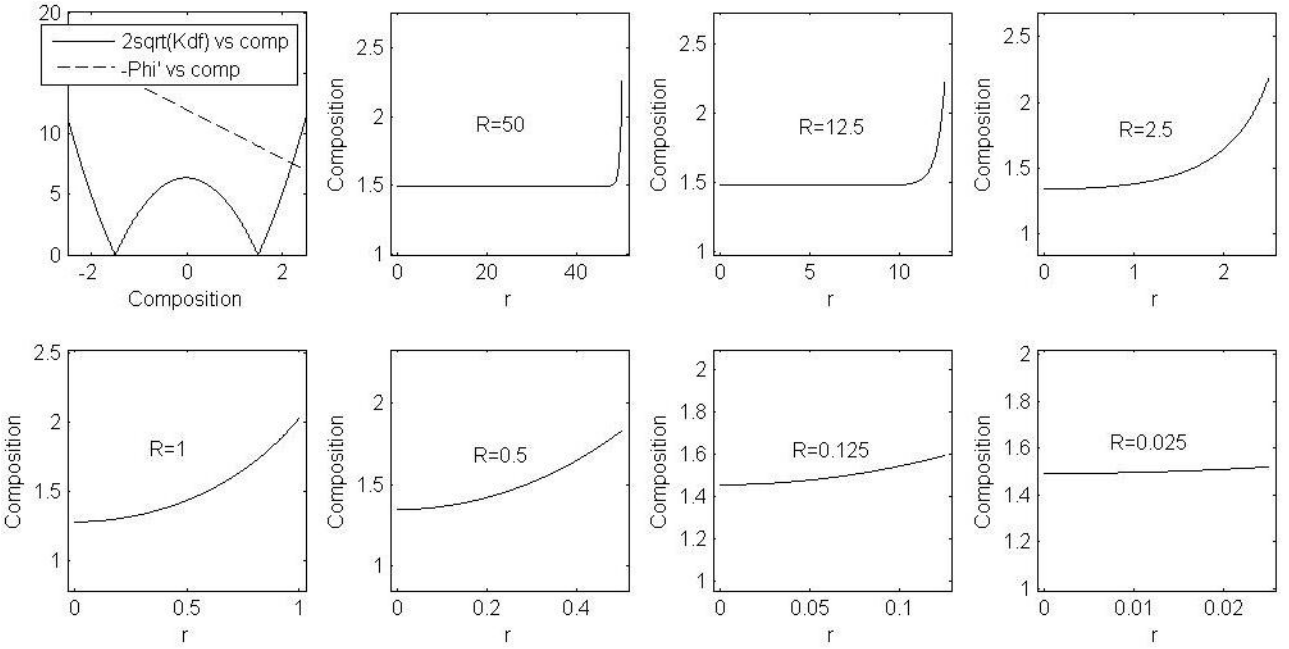

Figure 3.9: Composition profiles for an axisymmetric cylindrical free-film with an initial average composition of $c_{avg} = +1.5$

where $c_{avg} = +1.5$, there is no wetting of the unstable phase and the composition at the phase boundary is relatively higher than the initial average composition. The value of Φ_1 was chosen to better see how the composition at the phase boundaries and the composition in the bulk of the film are affected by the thinning of the film.

For the 1-D Cartesian case, the domain is gradually reduced from $L = 100$ to $L = 0.05$ using 1000 equally spaced nodes for each case. Similarly for the cylindrical case, the domain is gradually reduced from $R = 50$ to $R = 0.025$ with 1000 equally spaced nodes in between. The composition profiles are plotted against the thickness of the free-film. Figures 3.6 and 3.8 show the plot of the composition *vs.* the free energy function for which the results are derived and the composition profiles at various thicknesses of the film for the 1-D and the axisymmetric cylindrical cases respectively starting with $c_{avg} = -1.5$. Similarly, Figures 3.7 and 3.9 show the composition profiles for the 1-D and cylindrical cases respectively starting with $c_{avg} = +1.5$.

In Figures 3.6 and 3.8, it can be seen that the unstable phase at $c = -1.5$ wants to wet the phase boundary in all cases and there is no distinct jump between a wetting and a non-wetting condition. However, as the film becomes thinner and thinner, the mass constraint prevents the wetting phase to form. Also, in Figures 3.7 and 3.9, it is seen that the film prefers the composition at the intersection point of the curves $2\sqrt{Kdf}$ and $-\Phi'$ to wet the phase boundary, but the mass constraint prevents it from doing so.

3.4 Conclusion

In this chapter, numerical simulations have been performed that show in detail, the wetting of the gas-liquid phase boundary by a liquid phase that is not stable in the bulk of a free-film. This has been done in 1-D Cartesian coordinates and in an axisymmetric cylindrical geometry for different initial compositions and for various free energy contributions due to the free surfaces. A phase transformation of first-order is described and a jump from a wetting to non-wetting case or *vice-versa* has been shown. The effect of the film thickness on the composition profile of the free-film in which one phase wets the interface boundary was also examined. As the thickness of the free-film is reduced, the mass constraint imposed on the finite system prevents the unstable phase from wetting the interface boundary despite

the system desiring it. Thus, it can be concluded that for smaller systems of free-films, even though one might expect wetting to occur at the phase boundaries, it may not be seen due to the conservation of mass preventing it.

3.5 Future work

Future work under the conditions in which the system is close to the critical point requires the addition of fluctuations. Also, it might of interest to include the wetting effects in the development of the Navier-Stokes-Cahn-Hilliard equations for a free-film because the wetting of phases at the free surfaces will be affected by the hydrodynamics and stability of the free-film as well.

BIBLIOGRAPHY

[1] John Banhart, *Manufacturing Routes for Metallic Foams* 2000.

[2] John Banhart, Heiko Stanzick, Lukas Helfen and Tilo Baumbach, *Metal foam evolution studied by synchrotron radioscopy* 2000.

[3] Yu Gan and Van P. Carey, *Stability of thin free liquid films and the onset conditions for film rupture - A MD simulation study* 2007.

[4] A. McIntyre and L. N. Brush, *Spin-coating of vertically stratified thin liquid films* 2010.

[5] T. G. Myers, *Thin films with high surface tension* 1998.

[6] Alexander Oron, Stephen H. Davis and S. George Bankoff, *Long-scale evolution of thin liquid films* 1997.

[7] Thomas Erneux and Stephen H. Davis, *Nonlinear rupture of free films* 1993.

[8] A. De Wit, D. Gallez and C.I. Christov, *Nonlinear evolution equations for thin liquid films with insoluble surfactants* 1994.

[9] S. Tabakova and S. Radev, *On the Stability of a Free Viscous Film* 2008.

[10] S. Tabakova, *Dynamics and Stability of Free Thin Films* 2010.

[11] Ashutosh Sharma, C. S. Kishore, S. Salaniwal and Eli Ruckenstein, *Nonlinear stability and rupture of ultrathin free films* 1995.

[12] Martine Prevost and Dominique Gallez, *Nonlinear rupture of thin free liquid films* 1986.

[13] Bing Dai and L. Gary Leal, *Disjoining pressure for nonuniform thin films* 2008.

[14] Uwe Thiele, Santiago Madruga and Lubor Frastia, *Decomposition driven interface evolution for layers of binary mixtures. I. Model derivation and stratified base states* 2007.

[15] Santiago Madruga and Uwe Thiele, *Decomposition driven interface evolution for layers of binary mixtures. II. Influence of convective transport on linear stability* 2009.

[16] Lennon O Naraigh and Jean-Luc Thiffeault, *Nonlinear dynamic of phase separation in thin films.* 2010.

[17] John W. Cahn and John E. Hilliard, *Free Energy of a Nonuniform System. III. Nucleation in a Two-Component Incompressible Fluid* 1959.

[18] John W. Cahn, *Critical point wetting* 1977.

[19] M. R. Moldover and John W. Cahn, *An Interface Phase Transition: Complete to Partial Wetting* 1980.

[20] P. Tarazona, M. M. Telo da Gama and R. Evans, *Wetting transitions at fluid-fluid interfaces I. The order of the transition* 1983.

[21] I. Hadjiagapiou and R. Evans, *Adsorption from a binary fluid mixture. The composite wetting film at the solid-vapour interface* 1985.

[22] K. D. F. Wensink and B. Jerome, *Dewetting Induced by Density Fluctuations* 2001.

[23] H. Wang, R. J. Composto, E. K. Hobbie and C. C. Han, *Multiple Lateral Length Scales in Phase-Separating Thin-Film Polymer Blends* 2001.

[24] J. Genzer and E. J. Kramer, *Pretransitional thinning of a polymer wetting layer* 1998.

[25] John W. Cahn and John E. Hilliard, *Free Energy of a Nonuniform system. I. Interfacial Free Energy* 1958.

[26] P. G. de Gennes, *Wetting: statics and dynamics* 1985.

[27] Kevorkian J. and Cole J.D. *Perturbation methods in applied mathematics.* Springer 1985.

[28] John W. Cahn, *On Spinodal Decomposition* 1961.

[29] John W. Cahn, *Phase Separation by Spinodal Decomposition in Isotropic Systems* 1965.